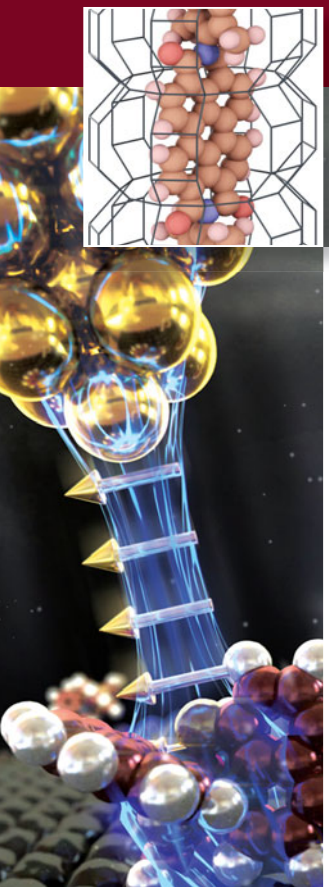

Intrinsic magnetic field effects in organic semiconductors

Markus Wohlgenannt, Peter A. Bobbert, and Bert Koopmans

The effects of a magnetic field on the current in sandwich devices of a nonmagnetic material in-between two ferromagnetic electrodes are well known. However, magnetic-field effects also occur in the responses of devices of organic semiconductors sandwiched in-between non-ferromagnetic electrodes, providing an entirely new route toward organic spintronics. The precise origins of these "intrinsic" magnetic field effects are still unclear. They appear to be related to spin-selective reactions between paramagnetic entities such as electrons, holes, and triplet excitons. We present an overview of these effects and discuss three recent developments that shed new light on them: (1) tuning of the effects in molecularly engineered systems, (2) the discovery of ultrahigh magnetoresistance in molecular wires, and (3) the discovery of "fringe-field" magnetoresistance.

Introduction: Organic electronics and spintronics

The two thriving technologies of organic light-emitting diodes (OLEDs)[1] and magnetoelectronics/spintronics[2] until recently had no overlap. However, over the last 10 years or so, there has been a growing realization that the class of materials that OLEDs are made from (i.e., organic semiconductors [OSCs]) show a number of interesting spin-dependent phenomena. This opens up the possibility that magnetoelectronic sensors and/or non-volatile logic gates could be fabricated from inexpensive plastic materials.

A basic OLED is composed of an OSC thin film sandwiched between an anode and a cathode. The feature that distinguishes OSCs from "ordinary" non-conductive plastics is the delocalization ("conjugation") of π electrons over the entire molecule, a feature familiar from the benzene molecule. As a result, a relatively small "forbidden energy gap" on the order of an eV separates the highest occupied and lowest unoccupied molecular orbitals (HOMO and LUMO, respectively). This is similar to the forbidden gap that separates the valence and conduction bands in inorganic semiconductors. However, disorder in the usually amorphous OSC layer prevents band transport. Instead, carriers hop incoherently from molecule to molecule.

Electrostatic forces pull holes and electrons—injected by the anode and cathode, respectively—together to form a "radical pair" (i.e., two spins located on neighboring molecules). By hopping onto the same molecule, the pair can form an exciton, either a spin-0 singlet (S, opposite spins) or a spin-1 triplet (T, parallel spins). T excitons typically have much lower energy than S excitons. The last statement follows from the Pauli exclusion principle: two spin-parallel electrons tend to avoid each other, therefore a hole (missing electron) is attracted to an electron with parallel spin. Electroluminescence occurs when the exciton decays radiatively.

In addition to electrostatic forces, charge carriers in OSCs also exert forces on each other mediated by vibrational fields. These forces are always attractive, even in electron-electron and hole-hole pairs. A single charge together with its vibrational field is called a "polaron" and a double charge a "bipolaron." The attractive force is usually not strong enough to lead to stable bipolarons, but bipolarons may occur as transient states. Like excitons, bipolarons can occur as singlets and triplets. However, different from excitons, the singlet bipolaron state is energetically favored.[3]

"Spintronics" deals with controlling and utilizing the electron spin degree of freedom (see the Introductory article in this issue). Giant magnetoresistive (GMR) devices use a change in the relative magnetizations of two ferromagnetic electrodes to control the current through a non-magnetic material.[2,4,5] The non-magnetic spacer layer can be a conductor[6–8] or a thin

Markus Wohlgenannt, Department of Physics and Astronomy, University of Iowa, USA; markus-wohlgenannt@uiowa.edu
Peter A. Bobbert, Eindhoven University of Technology, The Netherlands; P.A.Bobbert@tue.nl
Bert Koopmans, Department of Applied Physics, Eindhoven University of Technology, The Netherlands; b.koopmans@tue.nl
DOI: 10.1557/mrs.2014.132

insulator forming a tunnel barrier.[9,10] Utilizing semiconductors as spacer layers is particularly attractive because of the possibility of implementing spintronic logic devices. However, spin injection into semiconductors is challenging,[11] and the search for new materials systems is therefore ongoing. In particular, there has been increasing interest in using OSCs, in part due to their long spin relaxation times.[12,13] Organic GMR or "spin-valve" devices have been demonstrated, and these efforts are reviewed in the Nguyen et al. article in this issue.

Organic magnetoresistance

In addition to the organic spin-valve effect, there exists another magnetoresistive effect particular to OSC devices—organic magnetoresistance (OMAR).[14–17] In contrast to spin valves, OMAR devices do not require ferromagnetic electrodes, and the physics of this intrinsic magnetoresistance is completely different from that of spin valves. **Figure 1**a shows typical OMAR traces. These magnetoconductance traces were obtained by measuring a change in device current at a constant bias voltage as the applied magnetic field is varied. Most excitingly, OMAR occurs at room temperature, displays relatively large magnetoresistance of over 20% by applying small fields of just a few mT, and does so for a large variety of polymer and small-molecule devices. Experimentally, it has been established[15,18] that OMAR is approximately independent of the direction of the applied magnetic field B, and exhibits a characteristic Lorentzian-like response function, with a typical width of about 10 mT.

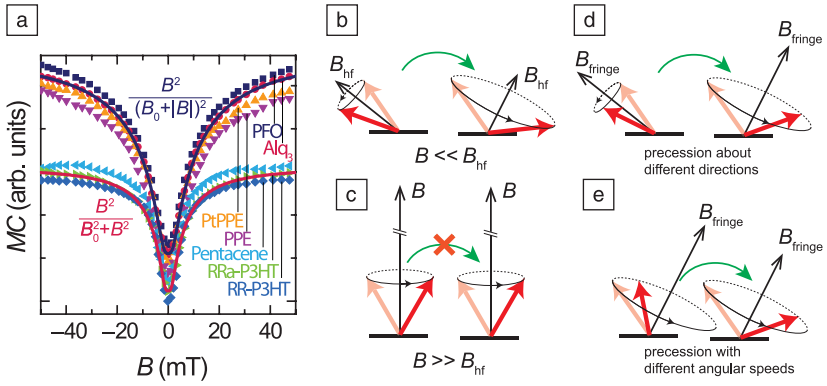

Figure 1. (a) Typical organic magnetoresistance (OMAR) traces (magnetoconductance *MC* versus applied magnetic field *B*) for a wide variety of polymer (PFO, PtPPE, PPE, RRa-P3HT, and RR-P3HT) and small molecule (Alq_3 and pentacene) devices, all showing either a Lorentzian ($B^2/(B_0^2 + B^2)$) or a specific non-Lorentzian ($B^2/(B_0 + |B|)^2$) dependence. For details, see Reference 18. (b–e) Pauli spin blocking in the formation of a singlet (S) bipolaron, after arrival of two charge carriers at neighboring molecules in a triplet (T) spin configuration (light colored red arrows). (b) When $B \ll B_{hf}$, the two spins precess about different hyperfine fields, mixing in S character, and bipolaron formation is possible. (c) When $B \gg B_{hf}$, the two spins precess about the same field B and remain in a T configuration (dark colored red arrows); bipolaron formation remains blocked. In the presence of fringe fields, lifting of the blockade can also take place because (d) they have different directions or (e) different magnitudes at the two molecules. Note: PFO, polyfluorene; PtPPE, platinum-containing polyphenylene-ethynelene; PPE, polyphenylene-ethynelene; RRa-P3HT, regio-random polythiophene; RR-P3HT, regio-regular polythiophene; B_0, characteristic magnetic field scale; B_{hf}, hyperfine magnetic field strength; B_{fringe}, fringe field of a ferromagnetic layer; Alq_3, 8-tris-hydroxyquinoline aluminum.

It is now believed that OMAR is akin to what are called magnetic field effects in spin chemistry,[19] a field that studies spin-selective reactions between spin-carrying, or paramagnetic, entities. In OSC devices, paramagnetic entities are present in the form of electrons, holes, and triplet excitons. Furthermore, as in spin chemistry, an important role is thought to be played by the hyperfine interaction. Hyperfine interaction refers to the coupling of the electronic and nuclear spins, for example, via a dipole-dipole interaction between the nuclear and electronic magnetic moments. In OSCs, a paramagnetic entity experiences a local hyperfine field (B_{hf}) on the order of mT, originating mainly from the hydrogen nuclei. This hyperfine field varies randomly from site to site and causes mixing between the spin states of a pair of paramagnetic entities on neighboring molecules. An externally applied field exceeding the hyperfine field suppresses this spin mixing and therefore changes the reaction rate between the entities. The relevance of hyperfine fields for OMAR has been demonstrated by targeted experiments comparing OMAR in ordinary and deuterated polymer devices.[20] However, what paramagnetic entities are involved and how OMAR is finally obtained is still being debated.

In order to explain why spin reactions affect the device current, we first discuss, in some more detail, one of the mechanisms put forward, dubbed the bipolaron mechanism.[3] As sketched in Figure 1b–c, we consider two neighboring molecules and suppose that two charge carriers of like charge have arrived at these molecules in a T configuration with aligned spins. If that is the case, a carrier on one of the molecules cannot hop to the other molecule into the same orbital as the other carrier because of the Pauli exclusion principle. Instead, it could hop into an energetically higher-lying unoccupied orbital, but there is an energy penalty on the order of an eV, and this will therefore not occur at room temperature. The resulting Pauli spin blockade prevents bipolaron formation. If, in addition, one of the two charges is immobile ("trapped"), then this spin-blockade shuts off any electrical conduction through this molecule.

When $B \ll B_{hf}$, precession of the spins about the different hyperfine fields at the two molecules mixes in S character, lifting the blockade in the course of time and allowing bipolaron formation, resulting in current flow (see Figure 1b). However, when $B \gg B_{hf}$, both spins precess around the same field B, and the carriers remain in a T configuration, preventing lifting of the blockade (see Figure 1c).

Apart from this bipolaron mechanism, two other kinds of mechanisms have been put forward as possible explanations for OMAR, which differ in the paramagnetic entities involved. (1) The electron–hole pair model,[16,21] in which the spin-selective reaction between oppositely charged polarons to form

an exciton—recombination—is of central importance. (2) The triplet exciton-polaron model,[22] which is based on the trapping of charges by triplet polarons.

Tuning OMAR by molecular engineering

Further understanding could lead to the next phase of OMAR research in which devices are tailored at will by design at the molecular level. Different approaches to control the flow of particles undergoing the relevant spin reactions can be imagined. As a specific example, blending semiconducting polymers with electron-accepting molecules has been demonstrated to provide a particularly attractive route for identifying the relevant mechanism(s) for OMAR.[23,24] This approach can profit tremendously from expertise built up from research on organic photovoltaics based on polymer/fullerene blends.[25]

Following pioneering work by Wang et al.,[23] Janssen et al. performed detailed studies on OMAR in blends of MDMO:PPV (a standard polyphenylene vinylene [PPV] derivative) with PCBM (a fullerene containing molecule) as a function of PCBM concentration and bias voltage.[24] The magnitude, sign, and line shape of the magnetoconductance (defined as $MC(B) = (I(B)–I(0))/I(0)$, where $I(B)$ is the current I at applied field B and $I(0)$ is the current at zero field) displayed pronounced changes over the studied regimes (**Figure 2**a–c). Careful analysis revealed that all three proposed mechanisms are relevant, albeit in different regimes. (1) In the pristine (hole-conducting) polymer devices, a relatively large, positive MC is observed, which is dominated by the triplet exciton-polaron mechanism. By adding just one percent of PCBM, the MC decreases dramatically (Figure 2b), explained by the strong quenching of excitons due to the high electron affinity of PCBM. (2) By increasing the PCBM concentration above 20%, the strongly reduced MC stays positive but is accompanied by a broad (~1 T) feature of opposite sign (Figure 2c). In this regime, electron-conducting percolative paths along fullerene molecules are formed, and a competition of formation and dissociation of charge transfer states at the PPV-PCBM interface promotes the electron–hole pair mechanism. The high-field effect of opposite sign is assigned to additional dephasing of electron and hole spins because of their slightly different gyromagnetic ratios (i.e., they precess at slightly different frequencies in the same magnetic field).[23] (3) Phase separation into PPV and PCBM regions occurs above 70%. This was found to be accompanied by a sudden sign change to a negative MC, while the high-field effect was quenched. This agrees well with a dominant bipolaron mechanism where only carriers of like sign meet in the respective phase-separated regions.

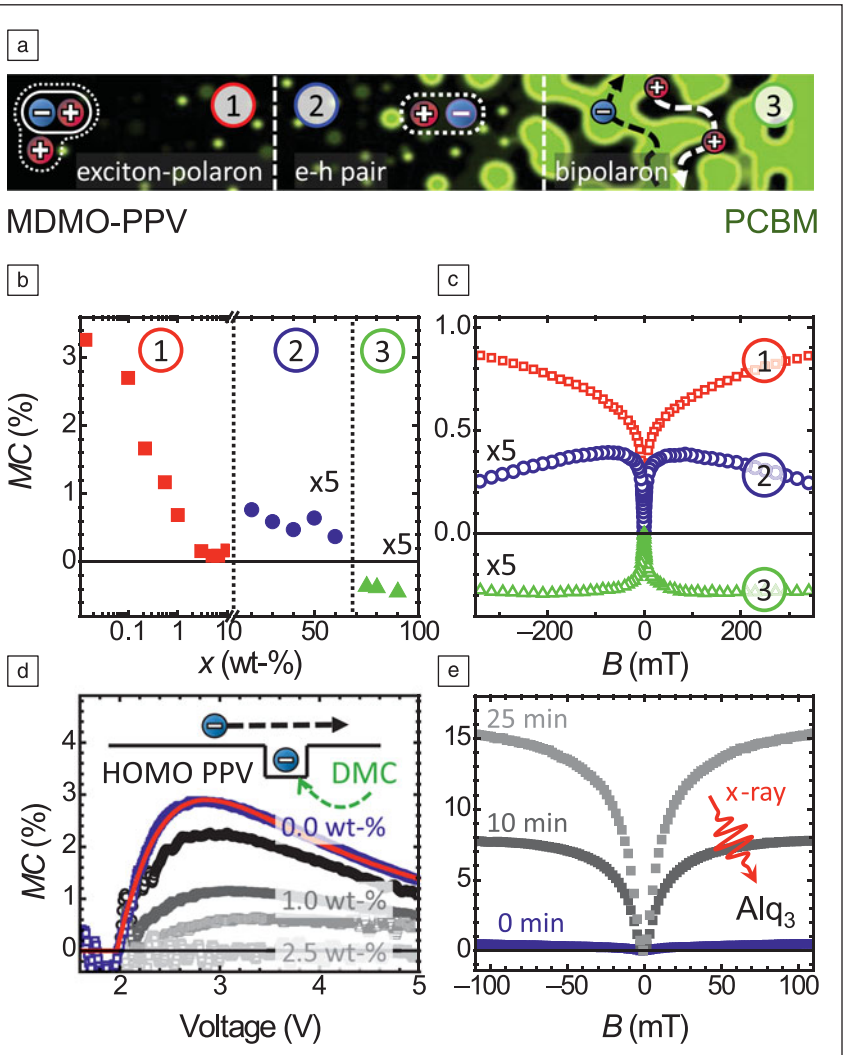

Figure 2. (a–c) Results for organic magnetoresistance on MDMO:PPV/PCBM blends, showing strongly contrasting behavior as a function of PCBM content x (in weight-%).[24] (a) Artist's impression of the blends in three regimes: (1) 0–20%, isolated PCBM (green) in PPV (black); (2) 20–70%, percolation of PCBM; and (3) >70%, phase separation into PPV and PCBM regions. The black (white) arrowed lines indicate the motion of electrons (holes) in the two continuous phases. (b) Sharp decrease in magnetoconductance (*MC*) after adding just a small fraction of PCBM, due to quenching of excitons, as well as a sign change to negative *MC* in regime (3). (c) Contrasting line shapes (*MC* as a function of applied magnetic field *B*) in the three regimes: (1, red) positive *MC*, (2, blue, multiplied by 5) positive low-field *MC*, with opposite high-field effect, (3, green, multiplied by 5) negative *MC* without high-field effect. (d) Quenching of *MC* in SY-PPV upon molecular doping by decamethylcobaltocene (DMC) molecules (increasing weight-% from upper to lower curve), known to deactivate electron traps (schematically illustrated in the inset).[26] Data show a characteristic dependence on voltage, fitted by a simple analytical model accounting for the role of trap filling on the triplet exciton-polaron mechanism (red curve). (e) *MC* traces for pristine and x-ray-exposed Alq_3 devices (exposure times indicated), showing the strong enhancement by introducing traps.[28] Note: HOMO, highest occupied molecular orbital; PPV, polyphenylene vinylene; MDMO:PPV, standard PPV derivative; PCBM, fullerene containing molecule; SY, super yellow; Alq_3, 8-tris-hydroxyquinoline aluminum.

In the regime of pure polymers, where effects are due to triplet exciton-polaron reactions as proposed by Gillin and co-workers,[22] the MC shows a very characteristic dependence on bias voltage, $MC(V)$ (Figure 2d). At low voltage, the MC is negligibly small, but rises sharply right at the so-called built-in voltage (V_{bi}) where internal fields in the devices are overcome, and the transport undergoes a transition from diffusive to drift character. At even higher voltages, the MC decays again. Cox et al. demonstrated[25] that such a behavior can only be accounted for by including the role of electron traps, omnipresent in these polymers.[26] Excitons formed by trapped electrons are thought to be far more efficient in binding free hole carriers, and thereby OMAR is governed by the magnetic field dependence of this trapped exciton density. While this density increases sharply above V_{bi}, its dependence on B is expected to decrease again once nearly all traps are filled at high voltage.

Actually, the importance of traps for OMAR was already known from earlier experiments. It is a common observation that the MC strongly increases when electrically stressing devices. More directly, Rybicki et al. showed that OMAR could be boosted by generating additional traps by x-ray irradiation[27] (Figure 2e). The reverse effect was demonstrated as well using molecular doping studies. Cox et al. molecularly doped super yellow PPV with decamethylcobaltocene (DMC), known to deactivate electron traps by donating electrons. Indeed, a reduction of the MC proportional to the DMC concentration was found (Figure 2d),[28] confirming the important role of electron traps for OMAR in bipolar devices.

Ultrahigh magnetoresistance in molecular wires

Rather than modifying molecular structures in thin-film devices, a complementary approach is provided by forcing molecules into one-dimensional architectures. Recently, ultrahigh room-temperature magnetoresistance was observed in molecular wires.[29] The present understanding is that this effect is an extreme expression of the Pauli spin blockade, explained previously (Figure 1b–c).

Figure 3a shows the measurement setup of Reference 29. The wires are formed by inserting a semiconducting molecule, DXP, into the pores of zeolite-L crystals. The crystals are contacted from below by a soft polymeric conductor and from the top by a conducting atomic force microscope tip. The experiments show that at low voltage, suppression of the current by a field of $B = 14$ mT to less than 5% of its value at $B = 0$ is possible, corresponding to a magnetoresistance $MR(B) = (I(0)–I(B))/I(B)$ of over 2000% (Figure 3b). The organic molecule DXP is known to easily accept two electrons[30] (negative bipolaron). The spin

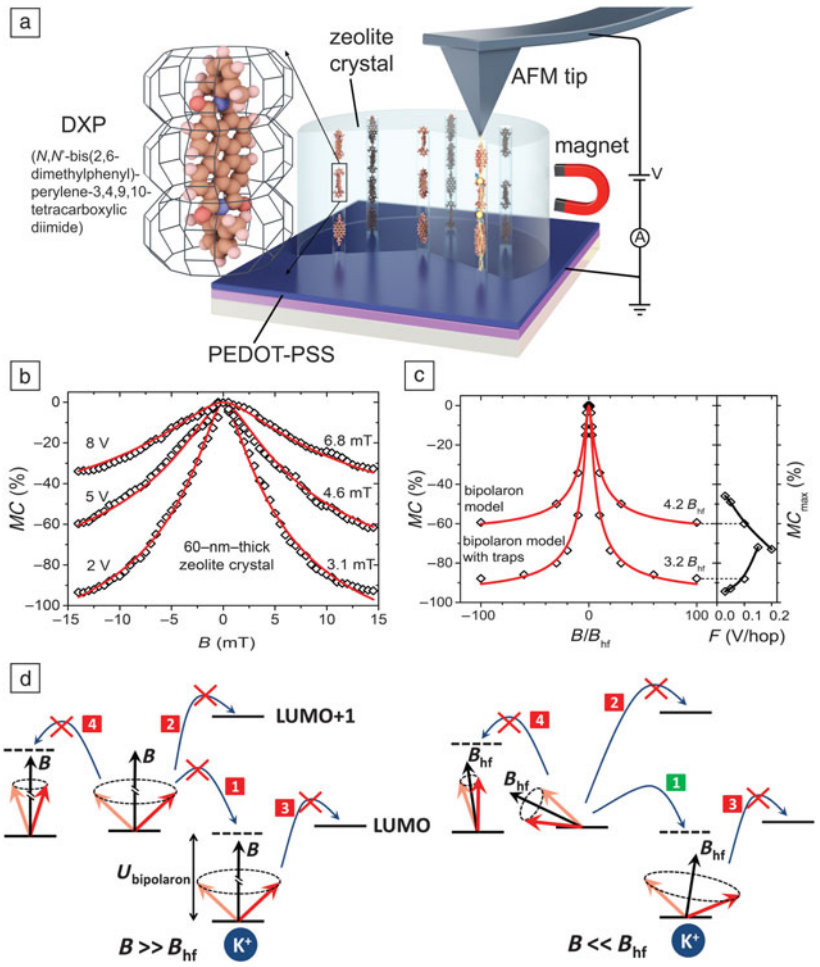

Figure 3. Ultrahigh magnetoresistance in molecular wires.[29] (a) Experimental setup. A zeolite-L crystal loaded with semiconducting molecules is contacted from below with a soft polymeric conductor (PEDOT-PSS) and from above with a conducting atomic force microscope tip (PtSi). In the structure of the molecule, the brown, white, blue, and pink spheres indicate C, H, N, and O atoms, respectively. (b) Measured magnetoconductance (MC) at different voltages of molecular wires in the channels of a 60-nm-thick zeolite crystal. Lines are fits to the organic magnetoresistance (OMAR) response function $\propto B^2/(|B| + B_0)^2$, with the indicated values of B_0. At 2 V, the current can be suppressed by the magnetic field to less than 5% of its value at $B = 0$. (c) Left: simulation results of the MC in a chain of 100 sites for a bipolaron formation energy $U_{bipolaron} = 0.2$ eV, an electron density of 0.3 carriers/site, and an electric field $F = 0.1$ V/hop, with fits to the OMAR response function. Results are shown for a Gaussian energy disorder with a standard deviation of $\sigma = 0.1$ eV and for a trap concentration of 0.15 traps/site with a trap energy $U_{trap} = -U_{bipolaron}$. Right: dependence of the maximal MC on electric field F. The simulations reproduce all main aspects of the experiment. (d) Explanation of the effect. Strong trapping of electrons occurs at molecules with a nearby potassium ion. Bipolaron formation, process (1), is forbidden for $B \gg B_{hf}$, but allowed for $B \ll B_{hf}$. Process (2) is not possible at room temperature because of the large energy difference between LUMO and LUMO+1. Process (3) is not possible due to the strong trapping. Process (4) is not possible due to Coulomb blocking. Note: LUMO, lowest unoccupied molecular orbital; B_0, characteristic magnetic field scale; B, applied magnetic field; B_{hf}, hyperfine magnetic field strength; MC_{max}, maximum observed magnetoconductivity.

blocking in this system will have a dramatic effect on the current since the charge transport is strictly one-dimensional, so there is no pathway around a blockade. This explains why the effect is so much stronger than bipolaron effects in bulk films, such as for $x > 70\%$ in Figure 2a–c.

Figure 3c shows simulation results using the same simulation technique as in Reference 3. The reason why the strength of the MC can exceed the –75% expected from the statistical fraction of formation of triplet radical pairs is that in the simulations, on top of spin blocking, strong Coulomb blocking also occurs. A detailed analysis of the simulations shows that the strongest low-voltage MC that can be obtained by a combination of spin and Coulomb blocking is –98.5%, corresponding to a magnetoresistance of 6000–7000%.[31] Figure 3d provides more details about what could be happening. Positive potassium ions are present in the zeolite pores to compensate for the negative charge of the aluminosilicate framework of the zeolite. Bipolaron formation will be favored by trapping at molecules with such an ion nearby.

Fringe-field organic magnetoresistance

OMAR is caused by spin interconversion in radical pairs—if for the two radicals, the local magnetic fields differ in direction (Figure 1d) or magnitude (Figure 1e), the relative spin-orientation of the radical pair evolves with time. Therefore, a critical ingredient to OMAR devices is a spatially varying magnetic-field landscape, which is usually provided by the molecular hyperfine fields. However, it can be beneficial to instead rely on an externally supplied magnetic field landscape. In that case, the response function of the OMAR traces can be engineered to match a desired application. Whereas OMAR sensors based on hyperfine magnetic fields are sensitive only in the 1–10 mT range, are non-hysteretic (i.e., they cannot sense the field's sign), and essentially isotropic (i.e., they cannot sense the field's direction), OMAR sensors based on an externally supplied field-landscape may overcome these limitations. Such "extrinsic" OMAR devices were recently demonstrated[32] using fringe fields emitted from a nearby ferromagnetic film as the source of the magnetic-field landscape. These fringe-field OMAR devices consist of a regular OMAR device fabricated directly on top of a ferromagnetic film (**Figure 4**a). To study the dependence of the device response on the distance separating the OMAR device and fringe-field source, a conducting polymer spacer layer of variable thickness was inserted between the OMAR device and the ferromagnetic film.

Magnetic fringe fields due to a ferromagnet are mainly determined by the magnetic domain structure. An image of the domain structure can be obtained by x-ray microscopy (Figure 4b) as a function of the applied magnetic field (the magnetization loop is shown in Figure 4c). Based on the domain images, a magnetostatic simulator was employed to calculate the fringe field distribution at any point above the magnetic film. This magnetic field distribution will determine the magnetoresistive response of the fringe-field OMAR device. The experimental MC traces are shown in Figure 4d. Figure 4e shows the results of a theoretical model (dotted lines) and a comparison with the experimental MC data (solid lines) for two spacer layer thicknesses, 15 nm and 100 nm. The model[33] takes into account the experimentally measured domain structure as a function of the applied magnetic field, and the range of the dotted line is limited by the available experimental images. The field dependence of the MC can be obtained from the model but not its magnitude. Nevertheless, the model reproduces the broadening of the magnetoconductance response and the shifting of the conductivity minimum away from zero B as the spacer layer thickness decreases.

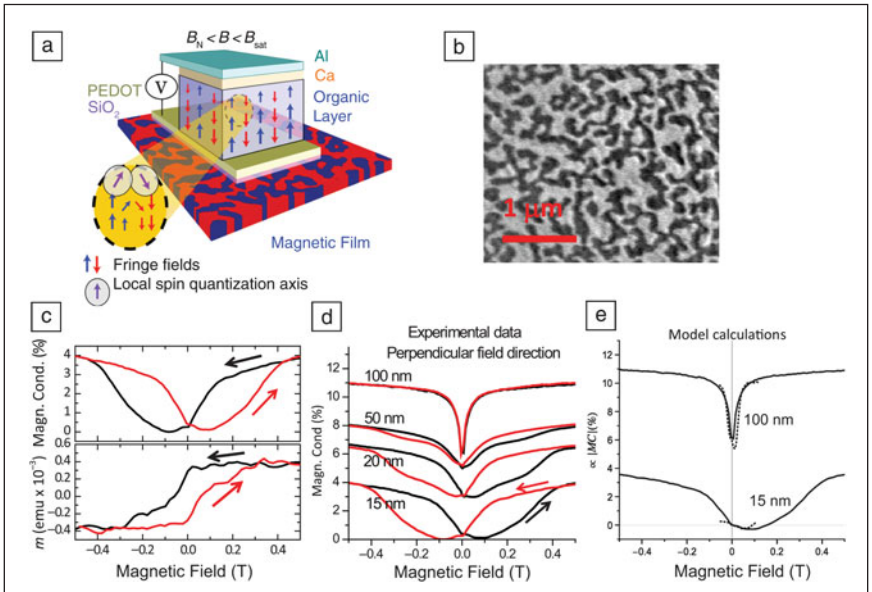

Figure 4. (a) Schematic of a fringe-field organic magnetoresistance (OMAR) device. The device consists of an organic magnetoresistive device fabricated on top of the ferromagnetic film, and separated from the latter by a spacer layer. (b) X-ray microscopy image of the domain structure of a Co-Pt multilayered ferromagnetic film. (c) Magnetoconductance (*MC*) (top) loop measured in a fringe-field OMAR device, and magnetization (*m*, bottom) loop for the film used in the device. The arrows indicate the direction of the field sweep. (d) *MC* measured in devices as a function of the spacer layer thickness. (e) Results of a theoretical model by Harmon et al.[34] for the *MC* (dotted lines) and comparison with the experimental data (solid lines) for two spacer layer thicknesses, 15 nm and 100 nm. The model takes into account the experimentally measured domain structure as a function of the applied magnetic field. The field range in which the model can be compared with experiment is limited by the available experimental images, but within this range, the model reproduces the main experimental features. Note: B, applied magnetic field; B_N, magnetic field strength at which domains nucleate; B_{sat}, magnetic field strength at which magnetization saturates.

Summary and outlook

Organic spintronics combines the thriving technologies of organic "plastic" electronics and magnetoelectronics/spintronics. Organic semiconductors are promising for spintronics applications because of their long spin relaxation times. Plastic spintronic devices can be fabricated using convenient solution-processing techniques. This is particularly true for devices based on the organic magnetoresistance (OMAR) effect, as they do not require ferromagnetic electrodes, but can, in principle, be constructed entirely from plastic (semi) conductors.

At the time of the first observations of OMAR about 10 years ago, it came as a surprise, and the underlying mechanism was poorly understood. Since then, much progress has been made. Indeed, it appears that OMAR research has now entered into a second phase, where molecular and supramolecular engineering is used to modify the OMAR device characteristics such as the magnetoconductance magnitude and the magnetic field range that it can sense. We have seen that in one-dimensional molecular wires, a small applied magnetic field of several tens of mT is sufficient to almost completely shut off the current flow. These are encouraging signs for the future realization of highly sensitive plastic magnetosensors and spintronic logic gates.

Acknowledgments

M.W. is indebted to his collaborators M.E. Flatté, A.D. Kent, F. Wang, F. Macia, and N.J. Harmon, and acknowledges financial support from ARO MURI Grant No. W911NF-08–1-0317 and NSF Grant No. ECS 07–25280. P.A.B. is indebted to his collaborators R.N. Mahato, H. Lülf, M. Siekman, S.P. Kersten, M.P. de Jong, L. De Cola, and W.G. van der Wiel, and acknowledges financial support from the Foundation for Fundamental Research of Matter (FOM), part of the Netherlands Organization for Scientific Research (NWO). B.K. acknowledges M. Cox, P. Janssen, and W. Wagemans for their contributions to this work, and financial support by the Dutch Technology Foundation STW and NWO-NANO.

References

1. R.H. Friend, R.W. Gymer, A.B. Holmes, J.H. Burroughes, R.N. Marks, C. Taliani, D.D.C. Bradley, D.A. Dos Santos, J.L. Brédas, M. Lögdlund, W.R. Salaneck, *Nature* **397**, 121 (1999).
2. S.A. Wolf, D.D. Awschalom, R.A. Buhrman, J.M. Daughton, S. von Molnár, M.L. Roukes, A.Y. Chtchelkanova, D.M. Treger, *Science* **294**, 1488 (2001).
3. P.A. Bobbert, T.D. Nguyen, F.W.A. van Oost, B. Koopmans, M. Wohlgenannt, *Phys. Rev. Lett.* **99**, 216801 (2007).
4. D.D. Awschalom, M.E. Flatté, *Nat. Phys.* **3**, 153 (2007).
5. M. Flatté, *IEEE Trans. Electron Devices* **54**, 907 (2007).
6. M.N. Baibich, J.M. Broto, A. Fert, F. Nguyen Van Dau, F. Petroff, P. Etienne, G. Creuzet, A. Friederich, J. Chazelas, *Phys. Rev. Lett.* **61**, 2472 (1988).
7. G. Binasch, P. Grunberg, F. Saurenbach, W. Zinn, *Phys. Rev. B: Condens. Matter* **39**, 4828 (1989).
8. M. Johnson, R.H. Silsbee, *Phys. Rev. B: Condens. Matter* **37**, 5326 (1988).
9. M. Julliere, *Phys. Lett. A* **54**, 225 (1975).
10. J.S. Moodera, L.R. Kinder, T.M. Wong, R. Meservey, *Phys. Rev. Lett.* **74**, 3273 (1995).
11. G. Schmidt, D. Ferrand, L.W. Molenkamp, A.T. Filip, B.J. van Wees, *Phys. Rev. B: Condens. Matter* **62**, R4790 (2000).
12. W.J.M. Naber, S. Faez, W.G. van der Wiel, *J. Phys. D: Appl. Phys.* **40**, R205 (2007).
13. V.A. Dediu, L.E. Hueso, I. Bergenti, C. Taliani, *Nat. Mater.* **8**, 707 (2009).
14. J. Kalinowski, M. Cocchi, D. Virgili, P. Di Marco, V. Fattori, *Chem. Phys. Lett.* **380**, 710 (2003).
15. T.L. Francis, O. Mermer, G. Veeraraghavan, M. Wohlgenannt, *New J. Phys.* **6**, 185 (2004).
16. B. Hu, Y. Wu, *Nat. Mater.* **6**, 985 (2007).
17. F.L. Bloom, W. Wagemans, M. Kemerink, B. Koopmans, *Phys. Rev. Lett.* **99**, 257201 (2007).
18. Ö. Mermer, G. Veeraraghavan, T.L. Francis, Y. Sheng, D.T. Nguyen, M. Wohlgenannt, A. Köhler, M.K. Al-Suti, M.S. Khan, *Phys. Rev. B: Condens. Matter* **72**, 205202 (2005).
19. K. Schulten, *Festkörperprobleme/Adv. Solid State Phys.* **22**, 61 (1982).
20. T.D. Nguyen, G. Hukic-Markosian, F. Wang, L. Wojcik, X.-G. Li, E. Ehrenfreund, Z.V. Vardeny, *Nat. Mater.* **9**, 345 (2010).
21. J.D. Bergeson, V.N. Prigodin, D.M. Lincoln, A.J. Epstein, *Phys. Rev. Lett.* **100**, 067201 (2008).
22. P. Desai, P. Shakya, T. Kreouzis, W.P. Gillin, N.A. Morley, M.R.J. Gibbs, *Phys. Rev. B: Condens. Matter* **75**, 094423 (2007).
23. F.J. Wang, H. Bassler, Z.V. Vardeny, *Phys. Rev. Lett.* **101**, 236805 (2008).
24. P. Janssen, M. Cox, S.H.W. Wouters, M. Kemerink, M.M. Wienk, B. Koopmans, *Nat. Commun.* **4**, 2286 (2013).
25. M. Cox, P. Janssen, F. Zhu, B. Koopmans, *Phys. Rev. B: Condens. Matter* **88**, 035202 (2013).
26. H.T. Nicolai, M. Kuik, G.A.H. Wetzelaer, B. de Boer, C. Campbell, C. Risko, J.L. Brédas, P.W.M. Blom, *Nat. Mater.* **11**, 882 (2012).
27. J. Rybicki, R. Lin, F. Wang, M. Wohlgenannt, C. He, T. Sanders, Y. Suzuki, *Phys. Rev. Lett.* **109**, 076603 (2012).
28. M. Cox, E.H.M. van der Heijden, P. Janssen, B. Koopmans, *Phys. Rev. B: Condens. Matter* **89**, 085201 (2014).
29. R.N. Mahato, H. Lülf, M.H. Siekman, S.P. Kersten, P.A. Bobbert, M.P. de Jong, L. De Cola, W.G. van der Wiel, *Science* **341**, 257 (2013).
30. S.K. Lee, Y. Zu, A. Herrmann, Y. Geerts, K. Müllen, A.J. Bard, *J. Am. Chem. Soc.* **121**, 3513 (1999).
31. S.P. Kersten, S.C.J. Meskers, P.A. Bobbert, *Phys. Rev. B: Condens. Matter* **86**, 045210 (2012).
32. F. Wang, F. Macia, M. Wohlgenannt, A.D. Kent, M.E. Flatté, *Phys. Rev. X* **2**, 021013 (2012).
33. N.J. Harmon, F. Macià, F. Wang, M. Wohlgenannt, A.D. Kent, M.E. Flatté, *Phys. Rev. B: Condens. Matter* **87**, 121203 (2013).
34. F. Macià, F. Wang, N.J. Harmon, A.D. Kent, M. Wohlgenannt, M.E. Flatté, *Nat. Commun.* **5**, 3609 (2014). □